The Astrophysical Journal, 627:L13–L16, 2005 July 1

RAPTOR OBSERVATIONS OF THE EARLY OPTICAL AFTERGLOW FROM GRB 050319

P. R. Woźniak, W. T. Vestrand, J. A. Wren, R. R. White, S. M. Evans, and D. Casperson
Los Alamos National Laboratory, MS-D466, Los Alamos, NM 87545; wozniak@lanl.gov, vestrand@lanl.gov, jwren@lanl.gov, rwhite@lanl.gov, sevans@lanl.gov, dcasperson@lanl.gov
Received 2005 April 9; accepted 2005 May 18; published 2005 June 9

ABSTRACT

The RAPid Telescopes for Optical Response (RAPTOR) system at Los Alamos National Laboratory observed GRB 050319 starting 25.4 s after γ-ray emission triggered the Burst Alert Telescope (BAT) on board the *Swift* satellite. Our well-sampled light curve of the early optical afterglow is composed of 32 points (derived from 70 exposures) that measure the flux decay during the first hour after the GRB. The GRB 050319 light curve measured by RAPTOR can be described as a relatively gradual flux decline (power-law index $\alpha = -0.38$) with a transition, at about ~400 s after the GRB, to a faster flux decay ($\alpha = -0.91$). The addition of other available measurements to the RAPTOR light curve suggests that another emission component emerged after $\sim 10^4$ s. We hypothesize that the early afterglow emission is powered by extended energy injection or delayed reverse-shock emission followed by the emergence of forward-shock emission.

Subject headings: cosmology: observations — gamma rays: bursts — shock waves

1. INTRODUCTION

Recent years have brought interesting developments in the domain of observations of the early optical emission from gamma-ray bursts (GRBs). Several groups now have the routine capability to respond to GRB triggers in real time using rapidly slewing robotic instruments (e.g., Akerlof et al. 2003; Bloom 2004; Boer 2004; Covino et al. 2004; Perez-Ramirez et al. 2004; Vestrand et al. 2002). Despite much effort in this area, so far only a handful of GRBs have been detected within the first minutes after the onset of the γ-ray emission, namely GRBs 990123, 021004, 021211, 030418, 041219a, 050319, and 050401 (e.g., Akerlof et al. 1999; Fox et al. 2003b; Woźniak et al. 2002; Li et al. 2003; Rykoff et al. 2004, 2005a, 2005b; Vestrand et al. 2004, 2005). Even fewer events have good signal-to-noise ratio (S/N) and coverage.

The discovery of the near-infrared transient from GRB 041219a (Blake & Bloom 2004; Blake et al. 2005) and its parallel detection in the optical band (Wren et al. 2004) expanded the list of known GRB properties. The RAPTOR (RAPid Telescopes for Optical Response; Vestrand et al. 2002) optical light curve of GRB 041219a (Vestrand et al. 2005) overlaps with the γ-ray emission by an unprecedented ~6.4 minutes. Vestrand et al. (2005) discovered a qualitatively new component of the early optical emission from GRBs and presented evidence for internal shocks (Mészáros & Rees 1999) as the emission mechanism. The presence of the new component was established on a purely empirical basis by its distinct close correlation with strongly time-varying γ-ray flux.

The updated taxonomy for GRB-related optical transient (OT) emission proposed by Vestrand et al. (2005) comprises (1) prompt optical emission contemporaneous with and consistent with a constant flux ratio to γ-rays (the ratio is $\sim 1.2 \times 10^{-5}$ in GRB 041219a [Vestrand et al. 2005]); (2) early afterglow emission that may start during the γ-ray emission and lasts for several seconds to minutes (uncorrelated with γ-rays and typically brighter than the prompt component; e.g., GRBs 990123 and 021211); and (3) late afterglow emission that emerges after the fading early afterglow and can persist for hours to many days (e.g., Fox et al. 2003a). The current theoretical framework offers, correspondingly, the internal-shock (Mészáros & Rees 1999), reverse-shock (Sari & Piran 1999; Panaitescu & Kumar 2004), and external-shock (Mészáros & Rees 1997; Sari et al. 1998) phenomena as a possible explanation of the observed properties.

In this Letter we present a comprehensive light curve of the early optical afterglow emission from GRB 050319 starting at 35 s after the GRB trigger.

2. OBSERVATIONS

On 2005 March 19, 9:31:18.4 UT (trigger time; hereafter $t = 0$), the Burst Alert Telescope (BAT) instrument on the *Swift* satellite (Gehrels et al. 2004) detected GRB 050319, a single-peak event with fast rise and exponential decay lasting $T_{90} \sim 10$ s (Krimm et al. 2005a, 2005b). The 15–350 keV fluence, the peak flux, and the photon index of the time-averaged spectrum were subsequently measured to be, respectively, 8×10^{-7} ergs cm^{-2}, 1.7 photons cm^{-2} s^{-1}, and 2.2 ± 0.2 (Krimm et al. 2005b). The on-board location (Krimm et al. 2005a) was distributed in near-real time through the GRB Coordinates Network (GCN) at 9:31:36.0 UT, $t = 17.6$ s.

Both the RAPTOR-S telescope and the RAPTOR-AB array responded to the alert. RAPTOR-S is a fully autonomous robotic telescope with 0.4 m aperture and typical operating focal ratio f/5. It is equipped with a 1K × 1K pixel CCD camera employing a back-illuminated Marconi CCD47-10 chip with 13 μm pixels. For technical details on RAPTOR-A and B see Vestrand et al. (2002).

RAPTOR-S was on target at 9:31:53.7 UT, $t = 35.3$ s. The rapid response sequence for RAPTOR-S consists of ten 10 s images followed by sixty 30 s images, a total of ~50 minutes of coverage (including the 15 s intervals between exposures used primarily for readout). A candidate OT at $\alpha = 10^{\rm h}16^{\rm m}47\overset{\rm s}{.}9$, $\delta = +43°32'54\overset{''}{.}5$ (J2000.0) was rapidly identified by Rykoff et al. (2005a) within half an hour. The OT was later confirmed by Yoshioka et al. (2005), and an absorption redshift $z = 3.24$ was reported by Fynbo et al. (2005). Initial analysis of the RAPTOR-S images (Fig. 1) showed that the OT was detected at high S/N in early exposures and gradually faded below the magnitude limit. Unfortunately, the observing conditions at the RAPTOR-S site during response were variable, and clouds obscured the field of view between $t = 1480$ and 2440 s.

The RAPTOR-B instrument responded slightly faster. Al-

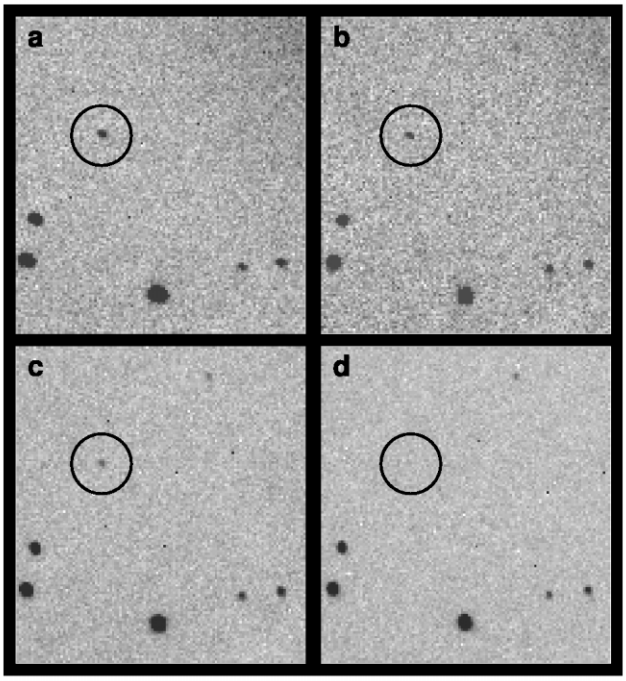

FIG. 1.—Examples of single RAPTOR-S exposures of GRB 050319; the OT discovered by Rykoff et al. (2005a) is circled. RAPTOR-S detected the OT with high S/N in the early 10 s frames (*a*, *b*), and followed its gradual decay down to the magnitude threshold of the 30 s frames (*c*, *d*) over the next 40–50 minutes. The size of the shown area is roughly 4.′5 × 4.′5, with north up and east to the left.

though none of those images is a detection, including the first 10 s frame starting at $t = 25.44$ s, the corresponding magnitude limit for OT is of some value (§ 4). RAPTOR-B and S are separated by about 37 km and have independent weather.

3. PHOTOMETRY

After standard corrections for bias, dark current, and flat-field responses, all frames underwent a 2 × 2 pixel binning. The binning was applied in order to bring the sampling of the stellar images to about the critical Nyquist value. In addition, it increased S/N per pixel and made the point-spread function (PSF) nearly circular.

We rejected 29 images taken between $t = 1480$ and 2440 s, when transparency was very poor due to passing clouds. In even later images the OT detections are marginal. We decided, therefore, to form two mean averages of 5 and 6 frames out of 11 images taken after $t = 2440$ s. A high S/N reference image was prepared by mean stacking twenty 30 s frames. All object centroids (including OT) were determined using the reference image. For the purpose of averaging and photometric analysis, all frames were resampled to a common pixel grid using a bicubic spline interpolator and a linear coordinate transformation with the ~0.08 pixel accuracy (rms) based on the positions of ~30 high S/N field stars. For image processing we used custom Difference Image Analysis software (Woźniak 2000).

PSF-weighted photometry within a 4 pixel radius was performed assuming a fixed centroid (from reference image) and without variance weighting. This general technique, used in the Sloan Digital Sky Survey (R. H. Lupton 2005, in preparation), hedges against a secondary nonlinearity between the bright and faint ends of the flux scale. It ensures that the much flatter variance profile of the background-dominated objects cannot propagate the systematic uncertainties from the PSF shape to the photometric offsets. We assumed a Gaussian PSF with FWHM = 6″ (2.44 pixels, binned). The flux scale with about 3.8% internal consistency was established using 11 high S/N stars in the vicinity of the OT. The calibration to standard *R* magnitudes was based on measurements of 22 USNO-A2.0 stars in the magnitude range $R2 = 12.5$–18.5. Residuals with respect to the best constant magnitude offset were random over the full flux range (good linearity) with rms scatter of 0.09 mag outside the photon noise–dominated region. Our unfiltered optical band has an effective wavelength close to that of the standard *R* band, but it has a larger width. For lack of the instrumental color information, we assumed that all objects have the color of a mean comparison star, i.e., $B - R = 1.25$ and $R - I = 0.73$, according to the USNO-A2.0 catalog. The fact that colors of the early GRB afterglows and their temporal evolution remain poorly constrained is a source of major uncertainty in transformations of broadband photometry (see § 4).

The early RAPTOR-B frame was analyzed using the same techniques as applied to the RAPTOR-S data. The actual limit was calculated by performing a fixed centroid PSF photometry at numerous random locations near the nominal OT position, taking the rms of the measured flux, and converting to magnitudes.

4. RESULTS

The final RAPTOR photometry of the early optical afterglow of GRB 050319 expressed on the *R*-band scale is given in Table 1. Figure 2 plots the light curve along with our model fits. Quimby et al. (2005) found an acceptable fit to an unfiltered optical light curve from the ROTSE-IIIb telescope using a single–power-law model with $\alpha = -0.59 \pm 0.05$. For the RAPTOR data the best-fitting single–power-law model has index $\alpha = -0.55 \pm 0.02$; however, it yields an unacceptable $\chi^2/\mathrm{dof} = 9.20$. A visual inspection of the RAPTOR measurements suggests a shallow flux decay at early times and significant steepening after ~400 s. In fact, the residuals with respect to the best-fitting single–power-law model are systematic and indicate a steepening trend. To test that hypothesis we fitted a broken–power-law model and obtained a reasonably good fit ($\chi^2/\mathrm{dof} = 2.91$) with $\alpha_1 = -0.38 \pm 0.03$, $\alpha_2 = -0.91 \pm 0.06$, and the break time $t_{\mathrm{br}} = 462 \pm 55$ s. It should be noted that instantaneous scale breaking in this direction may be hard to explain physically. Nevertheless, we find the model useful for investigating possible changes in the light-curve slope.

The residuals with respect to the best-fitting broken–power-law model appear flat; however, the reduced $\chi^2 = 2.91$ (81.42/28 dof) is still formally unacceptable. For some measurements the deviations from the best-fit model are well in excess of the error estimates; in particular, there are several strong outliers right near the fitted time of the break. There are also a few points with fluxes significantly larger than the model prediction right before passing clouds covered the field of view. The additional photometric scatter could be related to variable observing conditions and is discussed in more detail in § 5.

To establish the significance of the break, we fitted a series of broken–power-law models with a range of fixed break times. We found that the minimum of the χ^2 surface is not very well constrained and that the actual 68% confidence interval for the break time may be closer to ±100 s than to the formal parabolic error bar. Our conclusion is that the RAPTOR data indicate a significant steepening in the flux decay of GRB 050319 within the first hour after the γ-ray trigger. However, despite the appearance of sharp break in the light curve near ~400 s, our

TABLE 1
RAPTOR PHOTOMETRY OF GRB 050319

t_{start} (s)	t_{end} (s)	Δt_{exp} (s)	R (mag)	σ (mag)
25.4	35.4	10	>15.960	...
35.3	45.3	10	16.323	0.046
60.3	70.3	10	16.532	0.050
85.3	95.3	10	16.722	0.056
110.3	120.3	10	16.818	0.055
135.3	145.3	10	16.656	0.050
160.3	170.3	10	16.870	0.059
185.5	195.5	10	17.160	0.080
210.3	220.3	10	17.021	0.077
235.3	245.3	10	17.084	0.096
260.5	270.5	10	17.007	0.087
285.3	315.3	30	17.127	0.056
330.3	360.3	30	17.309	0.068
375.3	405.3	30	17.175	0.053
420.5	450.5	30	17.364	0.057
465.2	495.2	30	17.138	0.047
510.2	540.2	30	17.529	0.065
555.2	585.2	30	17.705	0.072
600.2	630.2	30	17.642	0.074
645.2	675.2	30	17.675	0.074
690.2	720.2	30	17.951	0.091
735.4	765.4	30	17.920	0.089
780.2	810.2	30	17.948	0.087
825.2	855.2	30	17.949	0.093
870.2	900.2	30	17.912	0.085
915.2	945.2	30	18.110	0.104
960.4	990.4	30	17.874	0.085
1005.2	1035.2	30	18.241	0.120
1050.2	1080.2	30	17.903	0.089
1095.2	1125.2	30	18.016	0.094
1140.4	1170.4	30	18.272	0.118
2445.0	2654.9	150	19.001	0.076
2669.9	2924.9	180	19.109	0.096

NOTES.—All measurements were obtained with the RAPTOR-S instrument, except for the limit at $t = 25$ s recorded by RAPTOR-B. Our unfiltered magnitudes were transformed to the R-band scale using the USNO-A2.0 catalog and were not corrected for extinction [Galactic $E(B - V)$ reddening is only 0.01 mag; Schlegel et al. 1998]. The last two images are stacks of five and six 30 s frames. For those images the effective exposure time accounts for readout breaks and is shorter than the difference between the end and start times ($\Delta t_{exp} < t_{end} - t_{start}$).

data are fully consistent with a gradual increase of the slope, possibly with additional small-scale photometric variations.

5. DISCUSSION

To test the robustness of the results of § 4, we reanalyzed the data using three other photometric tools to extract object fluxes, (1) traditional aperture photometry, (2) kernel matched difference image photometry (Woźniak 2000), and (3) a standard PSF package DoPHOT (Schechter et al. 1993), and obtained essentially identical light curves. While the steepening of the light curve and most wiggles were always present, the precise origin of the photometric outliers in Figure 2 still escapes explanation. Some comparison stars also show the wiggles, and some are fully consistent with the photon noise estimate. Li et al. (2003) noticed similar discrepancies in their light curve of GRB 021211 and suggested that color-induced systematics could be the cause. The intrinsic variability of the OT color or even a stationary color difference between the OT and comparison stars may generate systematic offsets in photometry. Given that the unfiltered spectral band is subject to a red atmospheric cutoff and weather variations during RAPTOR

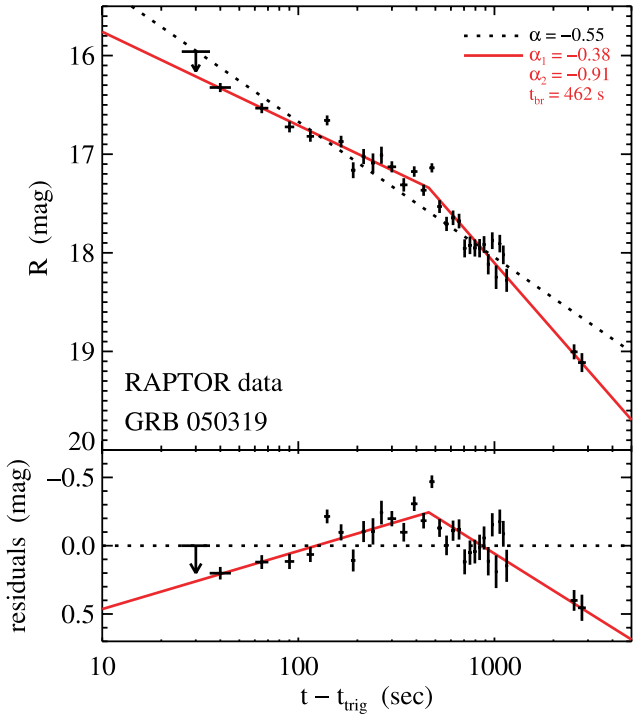

FIG. 2.—RAPTOR-S optical light curve of GRB 050319 (*top*) and photometric residuals with respect to the reference model (*bottom*). Our reference model, i.e., the best-fitting single power law (*black dotted line*), produces systematic residuals. We obtain a much better fit with a broken–power-law model (*red solid line*), which indicates significant steepening around ~400 s.

response, it is entirely possible that the outliers come from a systematic effect yet to be found. This experience underscores the importance of simultaneous color measurements of the early GRB afterglows using standard filters.

In Figure 3 we plot other OT measurements available at this time for comparisons with the RAPTOR light curve. The three points from the ROTSE collaboration (Quimby et al. 2005) were shifted by −0.04 mag to reflect the median difference between SDSS r and USNO-A2.0 R magnitudes for our comparison stars. The V-band points from *Swift* UVOT (Boyd et al. 2005) are plotted 0.7 mag brighter than actual values. All measurements reported in standard R band were taken at face value, since any finer issues with calibration to different catalogs should wait until the final revised photometry is available.

Measurements by other experiments agree with the shape of the RAPTOR light curve. While more sparsely sampled, the V-band light curve observed by the *Swift* UVOT (Boyd et al. 2005) also shows a faster flux decay after ~400 s. Further, the measurement at $t = 1.27$ hr by Yoshioka et al. (2005) is consistent with the extrapolated value predicted by the RAPTOR measurements. At times beyond ~1.3 hr, the published data from UVOT and other instruments show a transition back to a more gradual flux decay rate. The two breaks in the flux decay rate are visible in both the R-band and the V-band light curves. The close tracking between the light curves in both filters implies a constant $V - R$ color during the first day of the flux evolution. The zero point for the UVOT measurements is still not well established (Boyd et al. 2005), but taken at face value the reported measurements yield a color $(V - R) = 0.7$ for the OT counterpart of GRB 050319.

While the sample size is still small, one can already start to explore the morphology of GRB early afterglow light curves. The

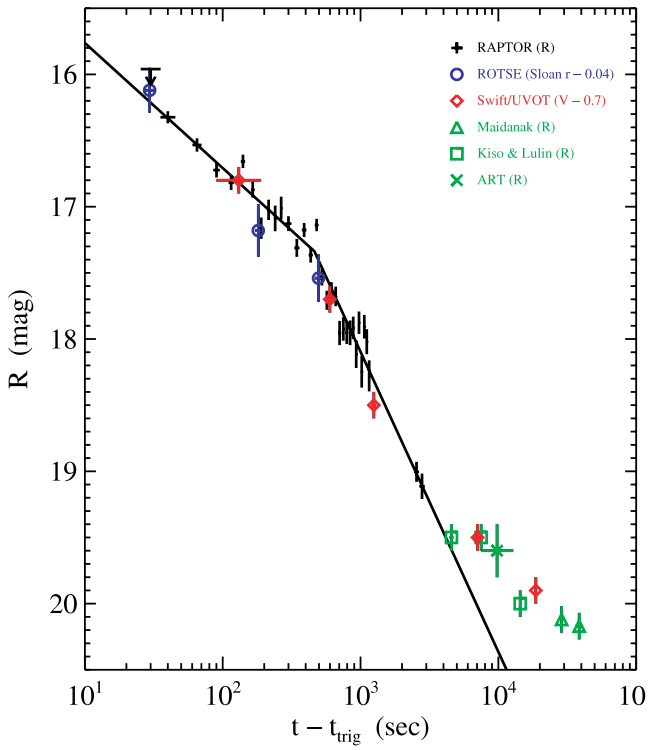

FIG. 3.—Comparison of the RAPTOR optical light curve of GRB 050319 with measurements from other instruments. The black points are RAPTOR measurements, while the data plotted in color are those obtained by other instruments: ROTSE (Quimby et al. 2005), UVOT (Boyd et al. 2005), Maidanak 1.5 m (Sharpov et al. 2005), Kiso & Lulin 1 m (Yoshioka et al. 2005), and ART 14 inch (Torii 2005). The line shows our best-fit broken–power-law model.

early afterglow behaviors of GRBs 990123 (Akerlof et al. 1999) and 021211 (Li et al. 2003) were very similar, with both OTs showing a steeper initial decline (power-law index $\alpha \simeq -1.8$) and the emergence of a shallower component ($\alpha \simeq -0.9$) after ~10 minutes. On the other hand, GRBs 021004 (Fox et al. 2003b) and 030418 (Rykoff et al. 2004) showed shallower initial decline (or even rise) with $\alpha > -0.6$ and then gradual steepening (to about $\alpha < -1.0$) on timescales of $\sim 10^3$ s or longer. The measurements we reported here for GRB 050319, starting from $\alpha_1 = -0.38$ and evolving to $\alpha_2 = -0.91$ after ~400 s, place its early afterglow properties in the latter group.

In the context of the standard fireball model, the shape of the optical afterglow light curve is determined by the nature of the interaction between the relativistic ejecta and the external medium. The relative importance and timing of the reverse- and forward-shock components, which depend on properties such as the density profile in the external medium and the strength of the magnetic field of the fireball, are reflected in the rates of flux evolution and the break times in the predicted light curve (e.g., Sari & Piran 1999; Mészáros 2002; Zhang et al. 2004). The morphology of the GRB 990123 and 021211 light curves, with the break to shallower decay, is usually attributed to the transition from the dominance of the reverse-shock generated emission to forward-shock generated emission (e.g., Li et al. 2003). For the more gradually decaying early afterglows, the interpretation is less clear. The gradually declining component could be associated with delayed reverse-shock emission (Vestrand et al. 2005) or an energy injection that continues well beyond the duration of the initial explosion (Fox et al. 2003b). The emergence of the additional component after $\sim 10^4$ s in GRB 050319 could then be understood as the emergence of the forward-shock emission. The prompt *Swift* localizations and rapid robotic follow-up are just starting to reveal the richness and complexity of the GRB afterglow phenomenology and, when combined with the models, will help to constrain the basic physical parameters of these cataclysmic explosions.

This research was performed as part of the Thinking Telescopes project supported by the Laboratory Directed Research and Development (LDRD) program at LANL. P. R. W. was supported by the Oppenheimer Fellowship.

REFERENCES

Akerlof, C., et al. 1999, Nature, 398, 400
———. 2003, PASP, 115, 132
Blake, C., & Bloom, J. S. 2004, GCN Circ. 2870, http://gcn.gsfc.nasa.gov/gcn/gcn3/2870.gcn3
Blake, C., et al. 2005, Nature, 435, 181
Bloom, J. S. 2004, GCN Circ. 2854, http://gcn.gsfc.nasa.gov/gcn/gcn3/2854.gcn3
Boer, M. 2004, Astron. Nachr., 322, 343
Boyd, P., et al. 2005, GCN Circ. 3129, http://gcn.gsfc.nasa.gov/gcn/gcn3/3129.gcn3
Covino, S., et al. 2004, Proc. SPIE, 5492, 1613
Fox, D., et al. 2003a, ApJ, 586, L5
———. 2003b, Nature, 422, 284
Fynbo, J. P. U., Hjorth, J., Jensen, B. L., Jakobsson, P., Møller, P., & Naranen, J. 2005, GCN Circ. 3136, http://gcn.gsfc.nasa.gov/gcn/gcn3/3136.gcn3
Gehrels, N., et al. 2004, ApJ, 611, 1005
Krimm, H., et al. 2005a, GCN Circ. 3117, http://gcn.gsfc.nasa.gov/gcn/gcn3/3117.gcn3
———. 2005b, GCN Circ. 3119, http://gcn.gsfc.nasa.gov/gcn/gcn3/3119.gcn3
Li, W., Filippenko, A., Chornock, R., & Jha, S. 2003, ApJ, 586, L9
Mészáros, P. 2002, ARA&A, 40, 137
Mészáros, P., & Rees, M. 1997, ApJ, 476, 232
———. 1999, MNRAS, 306, L39
Panaitescu, A., & Kumar, P. 2004, MNRAS, 353, 511
Perez-Ramirez, D., Park, H. S., & Williams, G. G. 2004, Astron. Nachr., 325, 667
Quimby, R. M., Rykoff, E. S., Schaefer, B. E., McKay, R., & Yost, S. A. 2005, GCN Circ. 3135, http://gcn.gsfc.nasa.gov/gcn/gcn3/3135.gcn3
Rykoff, E. S., Schaefer, B., & Quimby, R. 2005a, GCN Circ. 3116, http://gcn.gsfc.nasa.gov/gcn/gcn3/3116.gcn3
Rykoff, E. S., Yost, S. A., & Smith, D. A. 2005b, GCN Circ. 3165, http://gcn.gsfc.nasa.gov/gcn/gcn3/3165.gcn3
Rykoff, E. S., et al. 2004, ApJ, 601, 1013
Sari, R., & Piran, T. 1999, ApJ, 520, 641
Sari, R., Piran, T., & Narayan, R. 1998, ApJ, 497, L17
Schechter, L., Mateo, M., & Saha, A. 1993, PASP, 105, 1342
Schlegel, D. J., Finkbeiner, D. P., & Davis, M. 1998, ApJ, 500, 525
Sharapov, D., Ibrahimov, M., Karimov, R., Kahharov, B., Pozanenko, A., Rumyantsev, V., & Beskin, G. 2005, GCN Circ. 3124, http://gcn.gsfc.nasa.gov/gcn/gcn3/3124.gcn3
Torii, K. 2005, GCN Circ. 3121, http://gcn.gsfc.nasa.gov/gcn/gcn3/3121.gcn3
Vestrand, W. T., et al. 2002, Proc. SPIE, 4845, 126
———. 2004, Astron. Nachr., 325, 549
———. 2005, Nature, 435, 178
Woźniak, P. R. 2000, Acta Astron., 50, 421
Woźniak, P. R., et al. 2002, GCN Circ. 1757, http://gcn.gsfc.nasa.gov/gcn/gcn3/1757.gcn3
Wren, J., Vestrand, W. T., Evans, S., White, R., & Woźniak, P. 2004, GCN Circ. 2889, http://gcn.gsfc.nasa.gov/gcn/gcn3/2889.gcn3
Yoshioka, T., et al. 2005, GCN Circ. 3120, http://gcn.gsfc.nasa.gov/gcn/gcn3/3120.gcn3
Zhang, B., Kobayashi, S., Mészáros, P., Lloyd-Ronning, N. M., & Dai, X. 2004, in AIP Conf. Proc. 727, Gamma-Ray Bursts: 30 Years of Discovery, ed. E. E. Fenimore & M. Galassi (Melville: AIP), 208